

Review

Particle Size-Specific Magnetic Measurements as a Tool for Enhancing Our Understanding of the Bulk Magnetic Properties of Sediments

Robert G. Hatfield

College of Earth, Ocean, and Atmospheric Science, Oregon State University, 104 CEOAS Admin Building, Corvallis, OR 97331, USA; E-Mail: rhatfiel@coas.oregonstate.edu; Tel.: +1-541-737-3037; Fax: +1-541-737-2064

External Editor: Dimitrina Dimitrova

Received: 17 March 2014; in revised form: 11 October 2014 / Accepted: 21 October 2014 /

Published: 31 October 2014

Abstract: Bulk magnetic properties of soils and sediments are often sensitive proxies for environmental change but commonly require interpretation in terms of the different sources of magnetic minerals (or components) that combine to generate them. Discrimination of different components in the bulk magnetic record is often attempted through endmember unmixing and/or high resolution measurements that can require intensive measurement plans, assume linear additivity, and sometimes have difficulty in discriminating a large number of sources. As an alternative, magnetic measurements can be made on isolated sediment fractions that constitute the bulk sample. When these types of measurements are taken, heterogeneity is frequently observed between the magnetic properties of different fractions, suggesting different magnetic components often associate with different physical grain sizes. Using a particle size-specific methodology, individual components can be isolated and studied and bulk magnetic properties can be linked to, and isolated from, sedimentological variations. Deconvolving sedimentary and magnetic variability in this way has strong potential for increased understanding of how magnetic fragments are carried in natural systems, how they vary with different source(s), and allows for a better assessment of the effect environmental variability has in driving bulk magnetic properties. However, despite these benefits, very few studies exploit the information they can provide. Here, I present an overview of the different sources of magnetic minerals, why they might associate with different sediment fractions, how bulk magnetic measurements have been used to understand the contribution of different components to the bulk magnetic record, and outline

how particle size-specific magnetic measurements can assist in their better understanding. Advantages and disadvantages of this methodology, their role alongside bulk magnetic measurements, and potential future directions of research are also discussed.

Keywords: magnetic properties; environmental magnetism; magnetic susceptibility; magnetic grain size; sediment; particle size

1. Introduction

Magnetic properties of soils and sediments are among the most commonly made physical property measurements to understand records of past environmental change [1–12]. A simple suite of magnetic measurements can rapidly and non-destructively characterize the concentration, mineralogy, and magnetic grain size of magnetic minerals present in samples. These properties are strongly sensitive to the abundance and type of Fe-bearing minerals, which are both ubiquitous in environmental systems and sensitive to environmental change, such that magnetic measurements offer the opportunity to study temporal and spatial environmental variability in a range of settings. As a result, magnetic properties have been exploited in a variety of terrestrial, lacustrine, and marine environments to map anthropogenic pollution [13–15], investigate erosion, sediment sourcing and historical land use change [1,11,16–18], reconstruct paleorainfall estimates [19–21], map the incidence of ice rafted debris (IRD) [4,22,23] and dust [12,23,24] to the open ocean, understand the response of icesheets to climate [25], investigate ocean circulation [9,26–28], and document the cyclicity of Pleistocene climate in loess [29] and ocean sediments [24].

While sensitivity to multiple processes makes bulk (whole sample) magnetic measurements an attractive tool, it can also complicate interpretation. Identification of the process(es) driving the magnetic response in any particular record can be a non-trivial undertaking as magnetic concentration, grain size and mineralogy can be sensitive to geological variations [2,23], sediment particle size [11,30–32], sediment transport, delivery, and flux [4,7,9,25,26], anthropogenic pollution [13–15], and diagenetic [33–37], and authigenic [38–40] changes. When bulk magnetic properties are measured they often reflect this competition of different processes and magnetic mineral sources. If one process or source dominates, then interpretation of the drivers of magnetic properties is often easier than one experiencing multiple influences which can present a rather complex record. Interpretation is often achieved through correlation to independent variables, e.g., the abundance of lithic grains (e.g., >150 μm) if used as a proxy for IRD [4,41], heavy metals if tracking pollution [15,42], or sediment geochemistry for sediment fingerprinting and diagenesis [43–46]. However, the use of correlation in this manner often negates the advantages of exploiting magnetic properties in the first place; for example, why use magnetic susceptibility (MS) as a proxy for IRD if you have to physically count the IRD grains to qualify the magnetic proxy for them? Furthermore, inter-property correlations often sidestep addressing the more fundamental questions about what specifically drives magnetic property variations in any particular record. Lack of this understanding may be a major reason why magnetic measurements are often poorly understood and overlooked as potential investigative tools by the wider geoscience community.

When interpreting bulk magnetic properties, it is important to remember that they are rarely controlled by a single process or source. Instead, they are often the average of different magnetic mineral sources (termed components), each of which can potentially possess its own individual magnetic fingerprint. The aim for any environmental magnetic study should therefore be to try and identify the presence of different magnetic components and understand how in combination they influence bulk magnetic properties. In the literature, two main approaches have been utilized to try and unravel this complexity. The first approach attempts to unmix the signatures of different components using end members and/or through detailed examination of coercivity variances between components [47–55]. The second approach aims to characterize heterogeneity in the magnetic record and isolate different components through measurement of the magnetic properties of different sediment particle size constituents of the bulk sediment [10–12,17,30–32]. Both approaches have provided greater insights into what drives bulk magnetic properties in a variety of different environments, however, they are rarely employed in routine magnetic studies. Here, I discuss the origins of some different magnetic components in the bulk sediment record and how they can potentially be discriminated using both techniques. Then, as relatively underused, yet simple techniques, I shift to focus on the particle size dependence of magnetic properties and outline some important considerations when designing a particle size specific magnetic study, discuss their role alongside bulk magnetic property measurements, before finally providing an outlook and direction for future research.

2. Sources of Magnetic Minerals in the Environment

2.1. Sedimentary and Magnetic Properties

While all materials exhibit a response to an externally applied magnetic field ferrimagnetic minerals (e.g., magnetite, maghemite, titanomagnetite, pyrrhotite, and greigite) produce the strongest reactions and often dominate the magnetic properties of natural samples [2,56]. In their absence, weaker (canted-)antiferromagnetic minerals (e.g., hematite and goethite) and paramagnetic minerals (e.g., ilmenite, olivine, pyrite) can be important components in driving bulk magnetic properties [2,56]. These minerals largely originate from three sources; primary geological contributions, secondary neof ormation and alteration through processes of diagenesis and authigenesis, and tertiary contributions relating to anthropogenic pollution. Not to be confused with physical grain size, magnetic grain size is a fundamental magnetic property related to domain state. For magnetite (Fe_3O_4), one of the most common ferrimagnetic minerals in environmental materials, magnetic grain sizes are given as super-paramagnetic (SP < 0.03 μm), single domain (SD, 0.03–0.1 μm), pseudo single domain (PSD, 0.1–20 μm) and multi-domain (MD > 20 μm) for cubic and/or slightly elongated grains [57,58]. These size bounds can be expected to change with grain shape and mineralogy; for example, the upper SD limit for hematite is around 100 μm [59]. Differences in magnetic grain size and mineralogy are often discriminable in terms of the coercive force needed to (de)magnetize samples [2,56,60] and as such a variety of magnetic parameters have been developed to characterize and discriminate between them (e.g., [2,47,56,58,60]).

In terms of sediment grain size, magnetic grain size boundaries for magnetite naturally fall in the clay (<2 μm ; SP/SD, SD/PSD) and medium silt (16–32 μm ; PSD/MD) fractions while larger MD grains fall in the coarse silt (32–63 μm) and sand (>63 μm) fractions. For discrete magnetite particles, it might be

expected that differences in magnetic grain size exist between different sediment size fractions. However, magnetic minerals do not always exist as discrete entities and can often occur as inclusions within polycrystalline clasts. For example, basaltic glasses can be dominated by SP-SD grains [61] and medium to coarse silts can be dominated by relatively fine PSD size grains [32] complicating the seemingly simple and often assumed [9,27,28,62] scaling of magnetic and sedimentary granulometry. Understanding how sediment and magnetic grain size relate to each other is therefore important for interpretation, however, it is rarely considered in routine magnetic studies. Before discussing how to investigate this relationship, I will first discuss the origins of some common magnetic components that often contribute to bulk magnetic properties in environmental materials. This overview is intended to give an indication of the potential magnetic heterogeneity in environmental samples and how they might affect different sedimentary grain size ranges, not to evaluate the entire breadth of magnetic minerals in the environment. For further information and examples, see the excellent and detailed texts of Thompson and Oldfield [2], Maher and Thompson [63], and Evans and Heller [56].

2.2. *Origins and Properties of Different Magnetic Components*

Parent geology can provide a large proportion of the magnetic minerals to a soil or sediment often making it the dominant control on magnetic concentration, mineralogy, and magnetic grain size. Compounds of iron comprise roughly 5% of the Earth's crust and depending on fundamental controls such as geochemical composition and cooling rate [64,65], different iron-bearing minerals can grow to various sizes driving variances in magnetic mineralogy, concentration, and magnetic grain size. For example, red beds can get their distinctive coloring from hematite staining, iron sulphides can be the dominant magnetic minerals in slates, and ferrimagnetic iron oxides (e.g., magnetite, titanomagnetite) can constitute 2%–6% of basalts [2]. These magnetic mixtures are broken down via chemical, biological and, mechanical weathering to release both discrete and included magnetic minerals in a range clay, silt, and sand fractions into the environment. As a result, geological sources of magnetic minerals can often strongly dictate the magnetic properties of soils [3,66–68] and suspended [11], lake [1,69], and marine sediments [4,7,22–25]. If magnetic properties are assumed to be conservative [70] and maintain their geological fingerprints during sediment erosion, transport, and deposition, then magnetic discrimination of geological units can be exploited to facilitate sediment provenance studies [1,11,23,31,69].

While magnetic minerals are often assumed to be conservative in a range of settings, variation in environmental conditions can alter the reactive iron species within the mineral magnetic assemblage, potentially modifying their magnetic properties. Organic matter, pH, Eh, and sediment and porewater geochemistry are important factors that can promote reductive and/or oxidative diagenesis and authigenic (re)precipitation of magnetic mineral species that may differ significantly from those originally deposited. For example, given strongly reducing conditions, and excesses in porewater sulphate and organic matter [33,34,43] iron monosulphides (FeS), pyrite (FeS₂), greigite (Fe₃S₄), and ultimately pyrrhotite (Fe₇S₈), can form authigenically at the expense of magnetite and other reactive iron-(oxyhydr)oxides (e.g., goethite [FeO(OH)]). Commonly of relatively fine, magnetic grain size (SP/SD) [37,71–73], these species can be ferrimagnetic (e.g., greigite and pyrrhotite) or paramagnetic (e.g., pyrite) and constitute a significant portion of the magnetic mineral assemblage under favorable conditions. Similarly, oxygen rich environments can promote oxidation of magnetite to maghemite [74].

Dynamic sensitivity to variations in environmental conditions means that magnetic properties can reflect the non-stationarity of different processes, e.g., the formation of ferrimagnetic iron oxides on the surface of sapropels that were previously deposited under anoxic conditions [35,75]. Indeed, non-steady state conditions promoted during repeated wetting and drying cycles in soils are particularly important for the pedogenic formation and ferrimagnetic enhancement of soils in SP grains [38,67,76,77]. It is important to note that although redox state is an important factor dictating the nature of any diagenetic (or authigenic) change, the prevailing redox conditions do not necessarily result in alteration of the magnetic mineral population. The nature of any alteration (and its products) is constrained by the magnetic mineral species present in the sediment, their redox stability, biogenic activity and/or sediment geochemistry. However, significant alteration can strongly affect down core sediment bulk magnetic properties. For instance, during reductive diagenesis consumption of fine grained ferrimagnets and formation of paramagnetic pyrite can result in decreased magnetic concentration, an increase in paramagnetic concentration, and a coarsening of the magnetic remanence carrying components [33,44].

In addition to diagenetic consumption, oxidation and/or precipitation of magnetic minerals biological processes are capable of generating ferrimagnetic minerals. Magnetotactic bacteria can synthesize SD size magnetite and greigite into elongate chains and have been observed living throughout the sediment column or soil profile [39,40,78–80] sometimes forming a large remanence carrying component [79–83]. Possessing a relatively narrow coercivity range [49,50,52] magnetosomes are relatively well characterized magnetic components with First Order Reversal Curve (FORC) analyses particularly well suited to their identification [84–87]. However, as SD grain sizes are not unique to magnetosomes, it is still often necessary to confirm their presence using complementary techniques, e.g., transmission electron microscopy (TEM). Other natural processes including fire, lightning strikes, and in soils waterlogging and gleying can also have important influences on the stability and/or formation of different magnetic minerals resulting in changes in magnetic concentration, mineralogy, and magnetic grain size [3,66,67,88].

Tertiary contributions originate from a relatively narrow and specific range of sources related to ferrimagnetic particulates produced by industrial and vehicular exhausts. Often confirmed through scanning electron microscopy (SEM) and energy dispersive X-ray spectroscopy (EDS) discrete MD size spherules of magnetite can accumulate proximal to point sources [14,15,89]. These particles are often generated alongside, and strongly correlate with, other heavy metals and pollutants [43,88] making them a useful proxy for understanding the atmospheric dispersal of contaminants. Through measurement of the magnetic properties of tree leaves [15,89] and *in situ* surface sediments and soils [13,14] the extent and concentration of pollutants has been mapped from the individual road scale [14], through urban areas [90] and entire counties [91].

Different magnetic mineral species of SP, SD, PSD, and MD grains sizes can be generated by multiple processes and originate from multiple sources. Unfortunately, sources of different minerals are often not unique and/or confined to a single process or source, e.g., geology and bacterial magnetosomes can both produce ferrimagnetic SD size magnetite/maghemite. Therefore, for most environmental magnetic studies, the aim is often to discriminate between different minerals (e.g., magnetite and hematite) and grain sizes (e.g., SD/PSD/MD) that might relate to different processes. Aggregation of different components in the bulk sediment is responsible for the generation of the measured bulk magnetic properties of the sample. Discriminating the relative contribution of different components is therefore important for understanding the drivers of and processes involved in the generation of the bulk magnetic record.

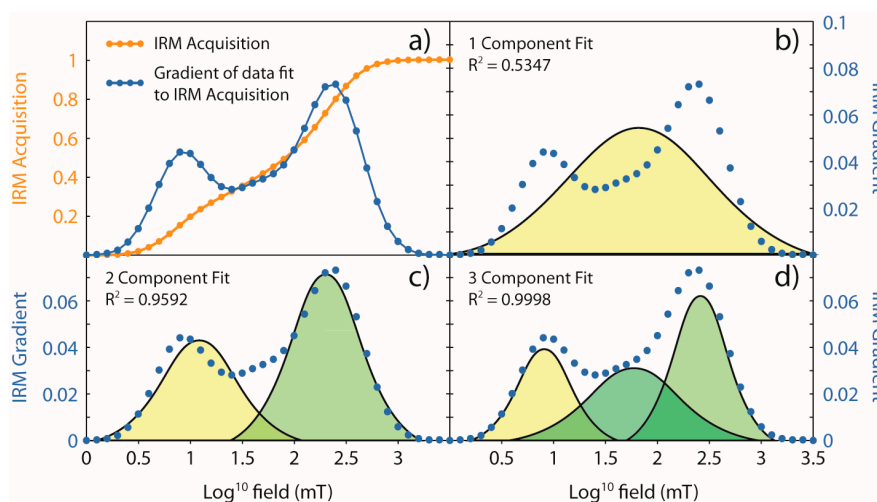
3. Unmixing Different Components Using Bulk Magnetic Measurements

If magnetic properties are assumed to be linearly additive and the different magnetic components that are present in the bulk sediment are distinguishable from one another, then potential exists to unmix their contributions within the bulk magnetic signal. Bivariate plots of two magnetic parameters provide a popular and relatively rapid method to visualize component mixtures. For instance, the Day plot [92] combines the ratios of the coercivity of remanence and coercivity (H_{cr}/H_c) to saturation remanence and saturation magnetization (M_{rs}/M_s) and is frequently used to help provide a semi-quantitative estimate of the average magnetic grain size of magnetite and the potential mixing of SP, SD, and MD contributions [93,94]. Similarly, the ratio of the mass normalized susceptibility of the Anhyseretic Remanent Magnetization (ARM) to mass normalized magnetic susceptibility (χ_{ARM}/χ) and the χ_{ARM} to mass normalized frequency dependence of susceptibility (χ_{ARM}/χ_{fd}) has been used to discriminate SD chains of bacterial magnetosomes from detrital catchment sources [31,95–97], while combinations of concentration independent ratios can be used to discriminate between different magnetic mineralogies [98]. If end-members of different sources or components can be defined then bivariate or multivariate unmixing can provide a quantitative estimate of the combination of different components [11,17,69,99]. For example, using catchment samples as source endmembers, Yu and Oldfield [69] used linear programming in an attempt to unmix source contributions in lake sediments [69]. In this example, lake sediments fall outside of the source endmembers which was interpreted to reflect inadequate source characterization and highlights the importance of endmember characterization for the linear unmixing of sediments [69,99,100]. In order to characterize end members for MD, interacting SD (ISD), uniaxial non-interacting SD (UNISD), and super-paramagnetic (SP) components, Lascau *et al.* [53] measured M_s , M_{rs}/M_s , the ratio of χ_{ARM} to the Saturation Isothermal Remanent Magnetization ($\chi_{ARM}/SIRM$), and the mass normalized susceptibility of the ferrimagnetic fraction (χ_f/M_s) [53]. Using the discrimination afforded by these magnetic grain size end members to represent different detrital, biogenic, and pedogenic components, they were then able to unmix the flux of different sources in lake sediments and discuss the potential processes responsible for driving temporal change [53,101].

Despite the breadth of different magnetic parameters, they can only discriminate the magnetic fraction in terms of their concentration, mineralogy, and magnetic grain size. This presents issues for linear unmixing as increasing the number of potential sources in mixtures increases the uncertainty in the result [98,100,102], with those results being increasingly non-unique [103]. As an alternative, high resolution measurements of ARM and/or IRM can be decomposed to reveal discriminable coercivity distributions that potentially relate to different components. Generation and optimization of the fit of a number of cumulative log Gaussian (CLG) functions to the changes in the slope of magnetic remanence acquisition or demagnetization curves can then be used to represent different components (e.g., [47,48,104,105]). Combinations of these distributions, each of which possessing a modal coercivity, dispersal range, and a relative proportion, can then be used to model the measured bulk magnetic properties (e.g., Figure 1). For example, the gradient of the IRM acquisition curve in Figure 1a is best modeled using three components (Figure 1d) which exhibits improved fit over the one- (Figure 1b) or two-component (Figure 1c) solution. This technique benefits from requiring no prior knowledge about a sample, however, the resulting distributions (*i.e.*, those in Figure 1d) then require interpretation in terms of the magnetic components they physically represent. While this approach is efficient at identifying high coercivity components

(e.g., hematite or goethite), from multiple lower and intermediate coercivity components (e.g., detrital and bacterial magnetite), discrimination of components with similar coercivity distributions can be more difficult [48,105,106].

Figure 1. (a) Isothermal Remanent Magnetization (IRM) acquisition curve (orange dots and line) and the gradient of the IRM (blue dots). One (b), two (c), and three (d) cumulative log Gaussian (CLG) distribution fits are shown to the data with their associated R^2 values. Note the greater fit of three CLG distributions to the IRM gradient data suggesting that the bulk magnetic dataset is best described as having contributions from three coercivity distinct components. Redrawn from Heslop *et al.* [48].

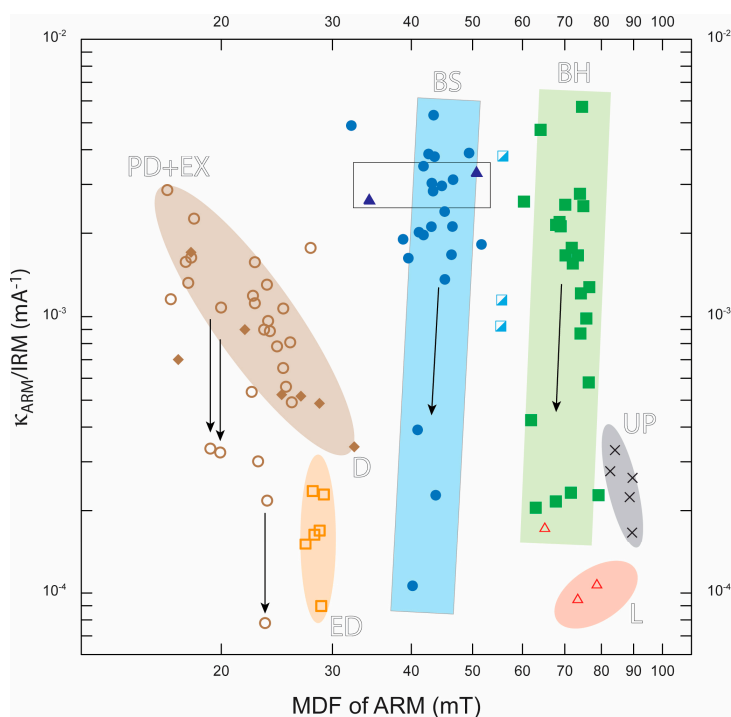


Furthermore, subsequent studies found CLG functions might not be the most appropriate representations of some magnetic components [49,50,106] which can often display characteristics that deviate from idealized Gaussian distributions [49,50]. Development of model functions that could incorporate non-Gaussian variation have shown to better fit and describe commonly occurring low-coercivity magnetic components [49–51] and performed better in identification of components with overlapping coercivity spectra [50,51]. These components can be summarized and discriminated using simple rock magnetic parameters (e.g., the median destructive field of the ARM (MDF_{ARM}) and volume normalized susceptibility of ARM to IRM (κ_{ARM}/IRM), Figure 2) providing the basis for discrimination of bacterial magnetosomes, extracellular and pedogenic ferrimagnets, detrital, eolian, and loessic components, and those signatures related to urban pollution from a range of environmental samples (Figure 2; [50–52,107–110]). Similar high resolution modelling approaches have been employed to unmix different shapes within hysteresis loops that relate to different magnetic components [55,111] and quantitative analysis of FORCs [84–86,112–114] are a useful tool to assess the nature, degree of magnetostatic interaction, and the abundance of different magnetic grain sizes within bulk samples [40,114].

Modeling and linear unmixing of the bulk magnetic signal is dependent on magnetic properties being linearly additive [48,50,53,99]. This may not always be a valid assumption in natural samples [99], particularly given the strong interacting nature of some components [40,53,101], that can promote strong non-linearity. However, the generally low concentration of magnetic minerals—and therefore greater dispersal of potentially interacting particles—in sediments compared to synthetic mixtures [99,100] or

concentrated magnetic extracts often makes this less of a concern in natural samples [50,115,116]. Interpretation of identified components often assumes a link between sediment and magnetic granulometry. For example, SD components are commonly assumed to be bacterial in origin, while MD grains are often interpreted as detrital contributions. This may be the correct assumption if magnetic fragments exist as discrete particles, but does less well in accounting for the potential of fine magnetic grains to be carried within larger polycrystalline clasts. These techniques also poorly characterize PSD grains often considering them as linear mixtures of SD and MD contributions in the bulk sediment [93,94] despite many natural samples being dominated by these magnetic grains [28,32,117–120]. Furthermore, detailed coercivity measurements can often require an intensive measurement program, sometimes utilizing specialized equipment that can make processing a large number of samples difficult [53]. However, despite these assumptions and limitations these techniques are extremely valuable for characterizing the magnetic heterogeneity inherent in bulk sediment samples.

Figure 2. Bi-plot summary of the median destructive field of the Anhyseretic Remanent Magnetization (MDF_{ARM}) and K_{ARM}/IRM clusters for different magnetic components as identified by Egli [50]. Letters classify and discriminate the different components into low-coercivity magnetosomes (biogenic soft, BS: blue dots and rectangle), high-coercivity magnetosomes (biogenic hard, BH: green squares and rectangle), ultra-fine extra cellular magnetite (EX: brown circles), pedogenic magnetite (PD: brown diamonds) and fluviually transported detrital particles (D: brown diamonds and brown ellipse), wind-blown particles (eolian dust, ED: orange squares), urban pollution particulate matter (UP: black crosses and ellipse), and maghemite in loess (L: red triangles and ellipse). The open rectangle intersecting BS relates to cultured magnetotactic bacteria (blue triangles); magnetosomes with intermediate coercivity fall between BS and BH clusters (open light blue half-filled squares). Arrows indicate the decrease of K_{ARM}/IRM observed during anoxic lake sediment conditions. All data redrawn from Egli [50].



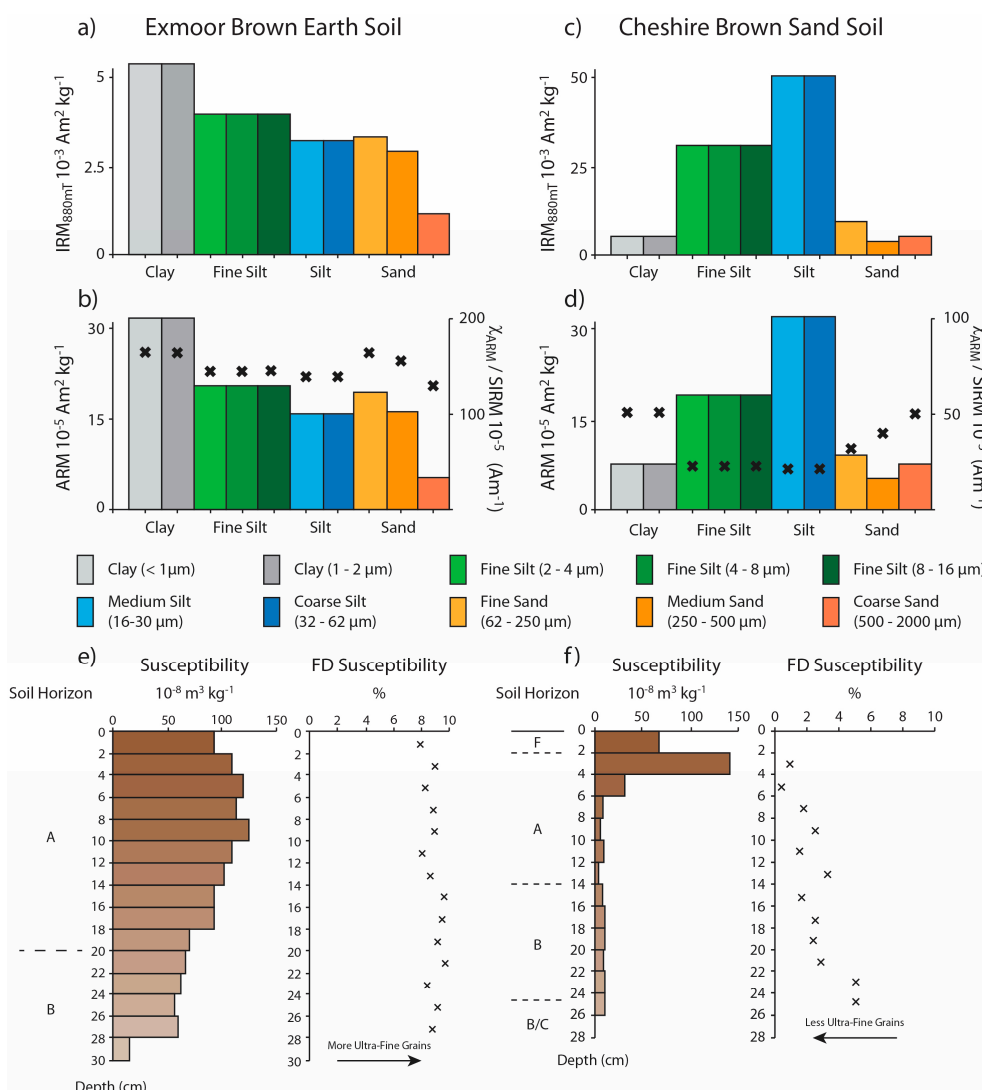
4. Particle Size-Specific Measurements

4.1. Origins of Particle Size Dependence

In contrast to unmixing of the bulk magnetic properties which exploit variations in concentration and/or coercivity, particle size-specific measurements inform on magnetic heterogeneity through the natural preferential association of different components with different physical grain sizes. When magnetic measurements are made on different size fractions they often reveal differences in the magnetic properties of different sediment size fractions [3,11,17,30–32,121–123]. Discrete magnetic grains might be expected to fractionate according to their physical size such that SP, SD, and fine PSD grains will likely reside in the clay fraction [31,121] and coarser PSD and MD grains in the silt and sand fractions [11,17,32]. If we assume different magnetic grain size populations reflect different components, then fractionation of the bulk sediment into different grain size bins can potentially isolate different processes and/or sources. This is neatly illustrated in the two soil profiles in Figure 3. Bulk MS is higher in the A horizon of both the brown earth and the brown sand suggesting ferrimagnetic enrichment in surficial layers relative to the sub soil, and high bulk frequency dependent susceptibility suggests the brown earth has a higher proportion of SP grains than the brown sand soil (Figure 3). Fractionation and measurement of different sediment particle sizes shows that ferrimagnetic grains are carried differently between fractions and between soil profiles. In the brown earth, highest MS and $\chi_{\text{ARM}}/\text{SIRM}$ occur in the clay fraction consistent with discrete SP/SD size ($\chi_{\text{ARM}}/\text{SIRM} > 100 \times 10^{-5} \text{ Am}^{-1}$; [3]) pedogenic magnetite [3,67]. High bulk MS in the surficial layers of the brown sand soil is associated with relatively coarse MD size ($\chi_{\text{ARM}}/\text{SIRM} \sim 20 \times 10^{-5} \text{ Am}^{-1}$; [3]) magnetic grains that are concentrated in the coarse silt fraction and relate to the atmospheric deposition of pollutants from combustion point sources [3,67]. In these soils, isolation and measurement of different size fractions quickly characterizes and discriminates how magnetic properties are carried in the bulk sediment, links their magnetic properties to sedimentology, and provides a method to discriminate them in the bulk sediment.

While PSD, MD and SP/SD domain boundaries occur within distinct sedimentological grain size classes the SP/SD domain boundary resides in the clay size fraction, over an order of magnitude below the fine silt—clay boundary ($\sim 2 \mu\text{m}$). It might therefore be anticipated that mixtures of SP/SD grains cannot be isolated by routine grain size fractionation. However, in an analysis of different pedogenic (dominantly SP-size) and bacterial (dominantly SD-size) magnetite dominated samples Oldfield *et al.* [31] showed that SD dominated grains regularly resided in a particle size class (e.g., 2–4 μm) larger than the SP dominated grains which often dominated the finest grades (e.g., $< 2 \mu\text{m}$). Discriminable on a bi-plot of χ_{ARM}/χ and $\chi_{\text{ARM}}/\chi_{\text{fd}}$ the reasons for this apparent differential association are not immediately clear, especially as the SD/SP domain transition is below 0.05 μm , but may relate to the aggregation of SD grains in magnetosome chains, their attachment to clay particles affecting settling velocity, and/or the inclusion of very fine PSD particles in the 0.2–2.5 μm range [31]. These results highlight not only the potential for discrimination of different sources using magnetic measurements—the authors suggest that 3 μm might be the optimum cut-off to isolate the pedogenic contribution—but that although discrete magnetic grain sizes largely scale with physical grain size, other factors (that are still not fully determined) can cause deviation from domain size bounds [31].

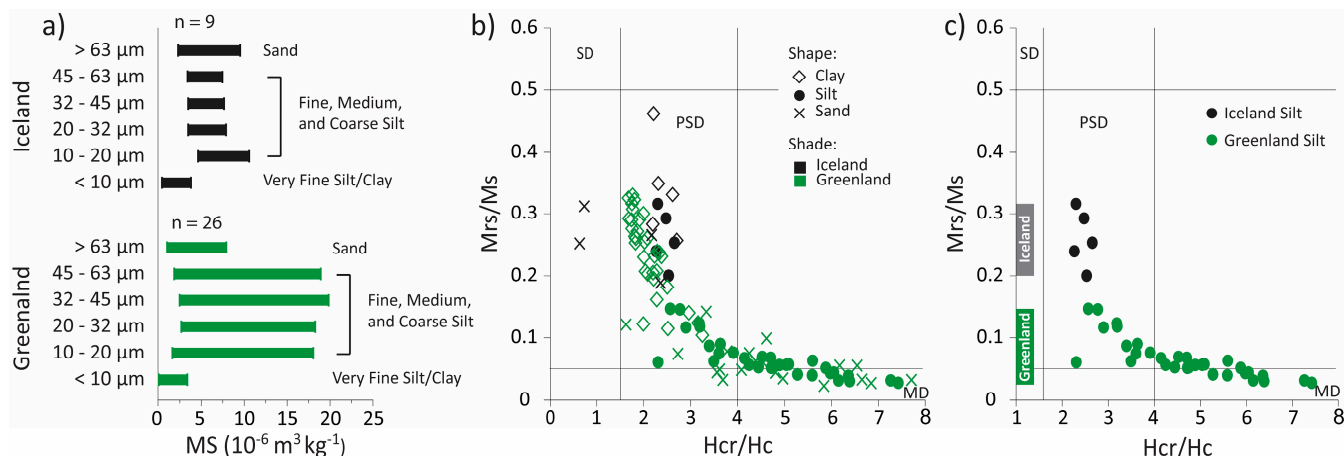
Figure 3. IRM, ARM, and $\chi_{ARM}/SIRM$ as a function of physical grain size for a Brown Earth (Cambisol) soil (a,b) and a Brown Sand Soil (c,d). Also shown are bulk MS and bulk frequency dependence of susceptibility with depth for the two soil profiles (e,f). Figure redrawn from Maher [3]. Note the $\chi_{ARM}/SIRM$ scale changes between profiles. The Exmoor Brown Earth soil has a relatively high percentage of ultra-fine pedogenic SP grains throughout the profile concentrated in the clay size fraction. In contrast, the brown sand soil carries its relatively coarse magnetic grains in the silt fraction and is restricted to the upper few centimeters of the profile resulting from atmospheric fall out of MD size ferrimagnetic pollution spherules.



Discrete magnetic components, e.g., magnetic spherules and bacterial and pedogenic magnetite, have relatively well defined magnetic properties and potentially preferential fractions they reside in. However, not all processes that affect the magnetic mineral population act in defined sedimentological ranges nor within certain magnetic domain bounds. The inclusion of magnetic minerals within polycrystalline clasts has significant implications for the interpretation of the magnetic record as it further decouples magnetic grain size from physical grain size. For example, in a comparison of glaciogenic sediments draining the Precambrian continental crust terranes of southern Greenland and oceanic basalts from Iceland magnetic

properties vary strongly both with source and sediment particle size (Figure 4, [32]). In both regions, ferrimagnetic minerals are concentrated in the silt fraction which possesses 2–5 times the MS of either the sand or clay fraction (Figure 4a, [32]). A Day plot shows that Icelandic clays, silts, and sands consistently contain relatively fine PSD sized magnetic grains (Figure 4b) while the magnetic grain-size of Greenlandic sediments scale with physical grain-size to a greater extent, so that the magnetic grain-size of the sand fraction is coarser than silt, which is coarser than clay. Only clay from Greenland contains magnetic grain sizes as fine as those sediments from Iceland [32]. Concentration of relatively fine PSD size grains in the Icelandic silt and sand fractions suggests that these grains occur as inclusions within larger polycrystalline clasts. As Iceland is dominated by extrusive mid-ocean ridge basalts [124,125], relatively rapid cooling rates may restrict the growth of larger magnetic grains. In contrast the intruded and metamorphosed continental crust of southern Greenland cooled over a longer period [126,127] potentially permitting growth of different magnetic grain sizes up to and including relatively coarse MD grains [32]. Upon weathering and erosion, this mixture of magnetic grains scales to a greater extent with physical grain size resulting in greater particle size dependence of magnetic properties. Incorporation of these different sources into sedimentary records has implications for their interpretation. For example, while magnetic grain size coarsening would accompany sedimentary grain size coarsening in Greenland sourced records and may be a useful paleo-current strength indicator [8,9,27,28], magnetic grain size proxies of Icelandic sourced sediment records would be less sensitive to changes in sediment grain size.

Figure 4. Variation of terrestrial magnetic properties with grain size: (a) Magnetic susceptibility (MS) (one standard deviation range about the mean) of six particle size fractions from Greenland and Iceland. Note how the MS of silts (10–63 μm) are 2–5 times higher than fine silt/clay (<10 μm) or sand (>63 μm) fractions. (b) Day plot (Day *et al.* [92]) of clay (<3 μm), silt (3–63 μm), and sand (>63 μm) fractions from Greenland (green data) and Iceland (black data). Note that all Icelandic fractions possess relatively similar fine pseudo single domain (PSD) magnetic grain sizes. In contrast, only Greenland clays possess the same magnetic grain size as Iceland samples, Greenland silts and sands fall further along the SD/MD (super-paramagnetic/multi-domain) mixing line possessing higher concentrations of coarser PSD and MD grains. (c) Silt data from (b) highlight the discrimination of source afforded by this fraction. Boxes on the y-axis show the range of Mrs/Ms values from different sources. All data from Hatfield *et al.* [32].

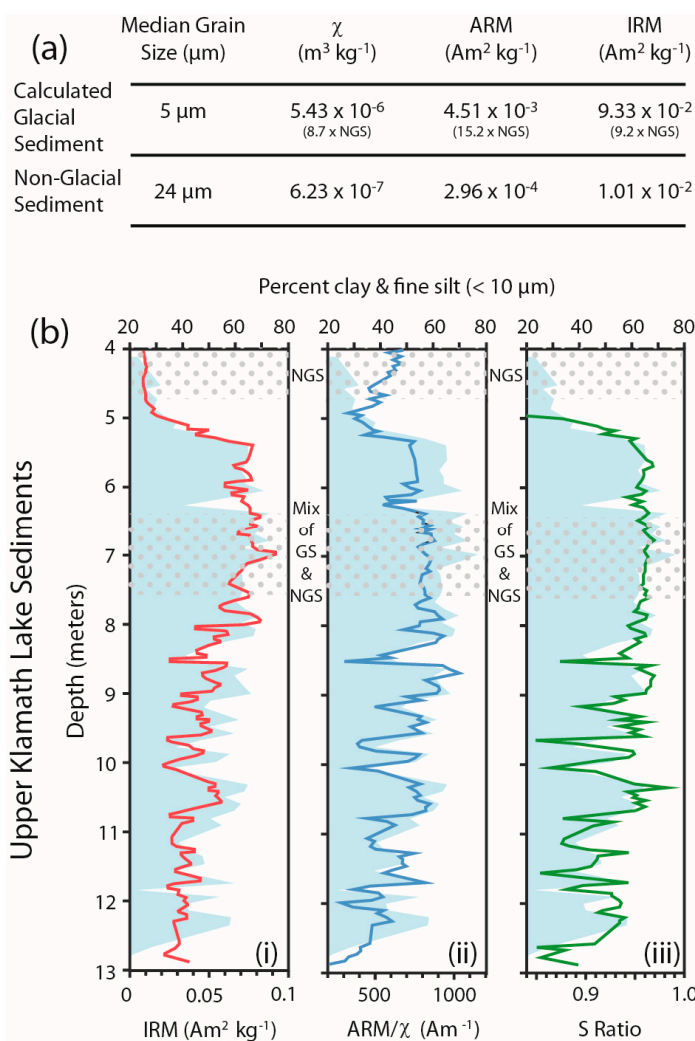


In addition to magnetic grain size variations, magnetic mineralogy can also possess strong particle size dependence especially if different fractions have different sources and/or transport mechanisms (e.g., [12]) The only way to investigate how the magnetic fraction is carried in the bulk sediment is through characterization of the different size fractions that constitute the bulk sediment sample. This methodology provides a way to examine what processes might be important in driving the bulk magnetic signal, which fraction it is held in, and how best to interpret changes in bulk properties that might occur both spatially and temporally. Furthermore, as sediment size in many environments is influenced by sediment transport processes, e.g., dust, bottom currents, or fluvial discharge, bulk magnetic properties can be sensitive not only to sediment source, but also to changes in sediment transport that control the availability and abundance of different fractions.

4.2. The Influence of Sediment Particle Size on Bulk Magnetic Properties

In many environments, different processes dictate the source, transport, and deposition of different physical grain sizes. For example, ice rafting during glacial periods can deliver otherwise absent terrigenous sand to the deep ocean, winnowing can dictate the spatial (and temporal) distribution of sediment particle sizes along current flow paths, turbidites have a characteristic upwards fining clastic signature, storms and catchment flooding can result in mobilization of large quantities of coarse sediment, and eolian sorting can often prescribe the physical grain size of loess. This information alone can be useful for understanding process, but if strong differences exist between the magnetic properties of different particle size fractions, then bulk magnetic properties can be strongly sensitive to changes in abundance of different sediment fractions within the bulk sediment. Assessment of the particle size dependence of magnetic properties and the sediment particle size distribution should be important considerations for the interpretation of bulk magnetic records where potential exists for strong variances in source and/or transport processes. For instance, let us consider a North Atlantic marine sediment core that receives sediment from both Greenland and Iceland. Terrestrial endmembers suggest that ferrimagnetic minerals are concentrated in the silt fraction (Figure 4). If these terrestrial properties are conservative through transport and deposition in the ocean, then small changes in the proportion of silt in the bulk sediment would be amplified in measurement of bulk MS potentially making MS a sensitive proxy for the amount of silt. This is the case in Upper Klamath Lake in Oregon where glacial flour with a median grain size of $\sim 5 \mu\text{m}$ is estimated to contain ~ 9 times the MS and a finer magnetic grain size than the non-glacially derived silt fraction (median grain size $24 \mu\text{m}$) (Figure 5a, [10,128]). Concentration of ferrimagnetic minerals in the finest fractions explains the strong coherence between changes in the proportion of fine grained silt and clay and bulk IRM (Figure 5b(i)) and helps establish the use of IRM as a proxy for the abundance of glaciogenic silt [128]. Magnetic mineralogy and magnetic grain size of the bulk sediment is also strongly biased by the ferrimagnetically strong, fine-grained, glaciogenic fraction. For example, changes in the proportion of the $<10 \mu\text{m}$ fraction in Klamath Lake sediments drives changes in bulk magnetic mineralogy and magnetic grain size that reflect the properties of the glaciogenic fraction (Figure 5a,b(ii,iii)) [128].

Figure 5. (a) Physical and magnetic properties of Upper Klamath Lake non-glacial sediment (NGS) (upper stippled zone in **(b)**) and the calculated glacial sediment end member (GS) from the mixed sediment (lower stippled zone **(b)**). Values in parentheses are the ratio of enrichment of magnetic properties in the GS compared to NGS, e.g., mass normalized MS (χ) of the GS is 8.7 times the value of the NGS. **(b)** Percent of sediment <10 μm (light blue shading) and **(i)** IRM (red line); **(ii)** ARM/ χ (blue line); and **(iii)** S-ratios (green line) for the Upper Klamath Lake sediment core [128]. Note the strong agreement between the amount of fine sediment (linked to higher proportions of glacial sediment) and bulk magnetic properties resulting from the concentration of ferrimagnetic minerals in the GS relative to NGS **(a)** in the mixed bulk sediment. All data from Rosenbaum *et al.* [128].



Instead of just a sum of different components, these results suggest that bulk magnetic properties should be considered as a convolved signal of the magnetic heterogeneity of different sediment size fractions (that is influenced by source(s)) weighted by their abundance within the bulk sediment (influenced by transport processes). While bulk magnetic properties are a convolved measure of the two, particle size specific measurements provide the opportunity to quantify the effect of both source and transport. Consideration of both factors has not always been the case in interpretation of bulk sediment magnetic records. For example, in marine sediment cores in the Northern North Atlantic (NNA) basin, source variability is traditionally assessed through measurement of bulk magnetic mineralogy, e.g.,

s-ratios to determine proportions of magnetically soft and hard components [4,9,22]. In this respect, our assessment of source may be hampered by an ability to easily discriminate between ferrimagnetic dominated sources (e.g., Iceland and Greenland, Figure 4). In practice, NNA records that do not display strong changes in bulk magnetic concentration or the proportion of high coercivity minerals (e.g., hematite) are generally assumed to possess a relatively homogeneous ferrimagnetic dominated source signature. Commonly dominated by PSD grains, these sediments are often assumed to be composed of discrete particles (e.g., [9,22,28]) with many ferrimagnetically dominated bulk magnetic grain size records interpreted in terms of sediment transport. For example, Mrs/Ms and the ratio of the volume normalized susceptibility of ARM to volume susceptibility (K_{ARM}/K) frequently used as proxies for variations in bottom current paleo-strength [26–28,62]. Recent data showing that ferrimagnetic grain size in the NNA can vary strongly with source (Figure 4) means that these previously transport related interpretations could instead be significantly influenced by source variations [32], especially in those records surrounding Iceland.

4.3. Isolation of Specific Components and/or Processes

If one magnetic component or process dominates the record then interpretation can be relatively simple (e.g., Figure 5). However, if the signal of interest resides in a fraction that is not abundant within the bulk sediment, and/or it is not reflected by a dominant magnetic component, then its signature can be overwhelmed by other fractions and/or components. If different components associate with different sediment fractions then isolation and measurement of specific grain size ranges can permit the targeting of specific processes and potentially amplification of non-dominant signals from the bulk magnetic record. For example, only the silt and sand fractions can discriminate Iceland and Greenland terrestrial sediments in Figure 4. As NNA sediment cores are often dominated by relatively fine silts and clays [27,129–131], magnetic grain size based source discrimination afforded by the silt and sand fractions would be diluted in the bulk magnetic record by the magnetic properties of the magnetically fine clay fraction (Figure 4). Isolation and measurement of magnetic properties of the silt and sand fractions provides the opportunity to view source variation free from the clay fraction which can vary in abundance depending on the efficiency of sediment transport.

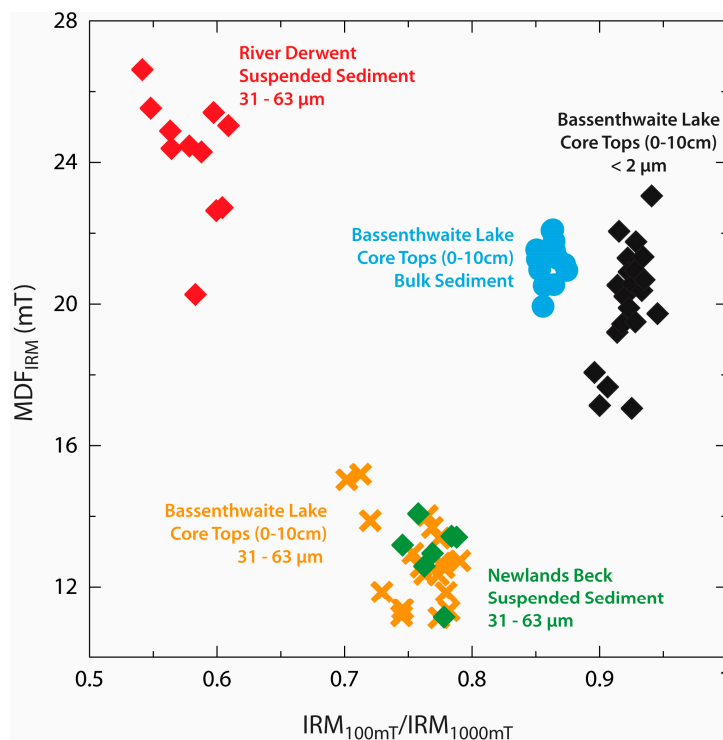
The association of different discrete and included magnetic grains with different sediment grain sizes potentially has implications for interpretation of the processes of post depositional alteration. In sediments that are affected by reductive diagenesis, it is usually assumed that the finest magnetic grain sizes undergo greatest alteration due to their greater surface/volume ratios. Selective dissolution of these (often assumed discrete) grains is usually given as the explanation for decreased magnetic concentration and the coarsening of average bulk magnetic grain size [2,43,45,132]. In a study of Senegalese shelf sediments affected by diagenesis, Razik *et al.* [12] examined the magnetic properties of 16 sediment size fractions. While all size fractions experienced some degree of alteration, the finest fractions showed a greater degree of change relative to the coarser fractions. This they suggest is explained by the greater surface area and reactive potential of the finest fractions, lower surface to volume ratios in the coarser sediments, and the potential protection afforded by magnetic grains being included within poly-crystalline clasts [12]. In cores less affected by diagenesis, the magnetic properties of different grain size ranges varied strongly with sediment grain size suggesting different source components could be isolated from

the bulk sediment [12]. The 10–63 μm fraction is characterized by relatively coarse magnetic grain sizes and lower S-ratios consistent with hematite rich eolian fractions sourced from the Sahara and Sahel, the ferrimagnetically rich <10 μm fraction possesses high concentrations of relatively fine magnetite grains interpreted to reflect delivery of fluvial sediments sourced from the Senegal drainage basin, while the magnetically weaker and coarser sands (63–500 μm) reflected the magnetic properties of marine carbonates [12]. While ferrimagnetic concentration is higher in the fine silt and clay fractions (<10 μm), the greater abundance of the 10–63 μm fraction makes silt an important contributor to bulk magnetic properties [12]. Variances in coercivity of these three different components could potentially be unmixed (see Section 3) to reflect their contribution to bulk magnetic properties. The added advantage of particle size specific measurements in this case is that the magnetic components can be interpreted in terms of their sedimentology and process; the hematite rich component occupies the modal grain size for eolian transport of Saharan and Sahel dust while the fine ferrimagnets in the <10 μm fraction are consistent with fluvial transport of igneous and/or pedogenic magnetite through the Senegal river [12]. Separation also allows the magnetically weaker hematite rich eolian fractions to be studied separately from the ferrimagnetically rich finer fluvial fractions that dominate bulk magnetic properties [12].

In addition to amplification of source and/or process, isolation of specific particle size ranges can also be used to negate the unwanted effect of certain sources of magnetic minerals. Bacterial magnetosomes are a common component in lake and marine sediments [11,31,39,40] that can often dominate bulk magnetic properties and overprint detrital fingerprints (e.g., [83]). These discrete SD grain size particles often reside in the finest fractions during separation [11,31], such that fractionation can isolate them from the detrital signature that might reside the coarser sediment fractions. Figure 6 shows this exemplified in Bassenthwaite Lake in Northwest England. Bassenthwaite Lake has two major sediment inflows, the River Derwent and Newlands Beck. The 31–63 μm fraction of suspended sediments originating from these two sources can be discriminated using IRM acquisition ratios and the MDF of IRM (Figure 6, [11]). The magnetic properties of the bulk sediment from the top 10 cm of four cores recovered from the lake are strongly influenced by that of the clay (<2 μm) fraction which are interpreted to be dominated by bacterial magnetosomes (Figure 6; [11]). When the coarse silt (and medium silt; 8–31 μm (not shown)) fraction in these core top sediments is isolated and measured its properties differ significantly from the bulk sediment and the clay fraction, falling on a mixing line between the coarse silt fraction of two inflow endmembers and suggests Newlands Beck forms the principal contemporary sediment source to Bassenthwaite Lake [11]. Linear unmixing of the bulk magnetic signal might have difficulty in correctly identifying the SD component as an additional magnetic source endmember. Particle size specific measurement reduces this problem to a two end member solution making for an easier assessment of sediment provenance.

In summary, particle size magnetic properties allows an assessment of how magnetic grains are carried in the bulk sediment sample. This methodology allows magnetic properties to be interpreted in a sedimentological context, allows an assessment of the influence of different processes on the bulk magnetic properties, and provides a pathway for amplification and negation of signatures that are potentially difficult to isolate and/or identify within the bulk measurements. However, like all analyses, they are not without their caveats and limitations, most of which pertain to the design and the implementation of their methodology.

Figure 6. Magnetic fingerprints for Bassenthwaite Lake core top sediments and catchment sources. Note how the bulk lake sediments (blue circles) have similar magnetic properties to the clay fraction (black diamonds) while the coarse silt fraction (orange crosses) differs significantly from these two falling on a mixing line between Newlands Beck (green diamonds) and River Derwent (red diamonds) suspended sediments. Isolation of the coarse silt fraction permits comparison with catchment inflows while the bulk magnetic properties are strongly influenced by bacterial magnetosomes that reside in the clay fraction. All data from Hatfield and Maher [11].



5. Designing a Particle Size-Specific Study

5.1. Number of Fractions

Choosing the optimal number and size range of fractions to separate from the bulk sediment is often the first question when designing any particle size specific study. Selection usually depends on several considerations including the research question(s) posed, the nature of the bulk sediment, the number of potential processes and sources, the time available, and the size of the bulk sample. A large number of separated fractions reduces the volume of material in each fraction and increases the time taken to make separations. This is an important consideration if initial bulk samples are small, or its properties are too weak to be reliably measured. While the current generation of Superconducting Quantum Interface Device (SQUID) magnetometers and Vibrating Sample Magnetometers (VSM) can measure remanence and in-field magnetic properties of small sediment samples relatively reliably, if this material is dominated by organic or other weakly magnetically material, as can be the case in many Holocene age lake sediment sequences (e.g., [133–135]), then sample volume becomes particularly important. Resources can also often dictate the number of fractions that can reasonably be generated from bulk samples. For example, separation of 16 fractions from 10 bulk samples quickly generates 160 samples for

measurement [12] that might require greater time and material commitments and potentially generates a tradeoff between the number of fractions and the number of samples that can be measured.

Balancing these considerations with the opportunities afforded by particle size specific measurement is therefore one of the central questions in any particle size study. Sometimes, a prior knowledge of process can be exploited to target specific particle size ranges, e.g., the modal grain size of Saharan dust (20–40 μm) [12], or the variation of magnetic properties in glaciogenic silt [10,32]. Other times, the focus on certain grain size ranges pertains to specific research questions, e.g., focusing on the finest fractions to understand the effect of pedogenesis and bacterial magnetosomes [31,122] or potentially understanding how diagenesis might affect different fractions [12]. Utilizing sedimentological information in this way is useful for targeting fractions that might most efficiently reveal and address the scientific research question(s) posed.

When *a-priori* knowledge of how magnetic properties may vary with physical grain size is not available, a sedimentological and/or bulk magnetic property pilot study may provide useful information for targeting fractions of interest. Grain size analysis of the bulk sediment can help identify the fractions most abundant and therefore those which might potentially contribute most to the bulk magnetic signal. While bulk magnetic measurements cannot directly identify the particle size dependence in the sample, they can provide an assessment of the average magnetic grain size and mineralogy and can potentially identify the presence of multiple components which might possess strong particle size dependence. For example, populations of SD sized magnetite that may be related to authigenic bacterial magnetosomes [50,51,112–114] are often identified through IRM acquisition and FORC analyses. With a relatively narrow coercivity range, and characterized as either magnetically hard (BH) or soft (BS) bacterial components (e.g., Figure 2, [49–52]), they often associate with the finest sediment fractions [11,31]. With knowledge of the abundance of the fine fractions, an experiment can be designed to examine how these components might affect the bulk magnetic record. Equally, if the coarser silt and sand fractions form a large part of the sample, then these fractions might also warrant more attention in the fractionation program. If no sample information is available, nor is the opportunity to perform a pilot study, then simple informed decisions about the nature of the sample can be the most useful approach. For example, in samples dominated by a relatively fine granulometry (e.g., soils, loess and eolian deposits, and suspended, lake, and marine sediments), separation into sand (>63 μm), silt (2–63 μm), and clay (<2 μm) fractions can be a very useful and informative first step. If silt turns out to be the dominant granulometric and/or magnetic fraction, it may then be advantageous to further separate this fraction into smaller grain size bins (e.g., [11,17,18,31,32]) as the silt fraction has often shown to be important for carrying a large proportion of the detrital bulk magnetic signal [3,10,11,32,128]. In the literature, the number of generated ranges from two or three up to 16, though commonly around 5–6 fractions are chosen with a focus on the clay, fine silt, and silt fractions [10–12,136,137]. However, ultimately the choice of the number of fractions is a balance between resources and study aims.

5.2. Sample Preparation

Several methods have been outlined in the literature to achieve fractionation of sediment samples [115,138–141]. The simplest and most frequently used involve a combination of sieving of the larger sediment fractions and settling/pipetting of the finer fractions according to Stokes Law. Samples

are often pre-treated with a dispersal agent (e.g., sodium hexametaphosphate, tetra-sodiumdiphosphate) to promote disaggregation of flocs in the fine silt and clay fractions. It is important to note the concentration and volume of any added dispersants as they ultimately reside in and contribute to the weight of the finest sediment fraction after settling. Wet sieving is most suited for separation of the sand and coarse silt fractions and is achieved by washing the dispersed sample through a sieve of pre-determined size. For relatively fine sediments, a 63 μm sieve can be used to obtain a sand fraction and, if required, the coarser silt fractions can be obtained using sieves with smaller openings down to about 20 μm (e.g., [32]). Settling is most suited to fractionate samples smaller than those that can be sieved, e.g., fine silts and clays. By making a few assumptions, we can exploit the different settling velocity speeds of differently sized particles according to Stokes' law.

$$V_t = \frac{gd^2(\rho_p - \rho_m)}{18\mu} \quad (1)$$

where V_t is the settling velocity ($\text{m}\cdot\text{s}^{-1}$), g is the acceleration due to gravity ($\text{m}\cdot\text{s}^{-2}$), d is the particle diameter (m), ρ_p and ρ_m are the density of the particle and the medium, respectively ($\text{kg}\cdot\text{m}^{-3}$), and μ is the viscosity of the fluid ($\text{kg}\cdot\text{m}\cdot\text{s}^{-1}$).

Assuming all other factors remain equal, settling velocity is largely determined by density which is dependent upon mass and ultimately particle size. Manipulation of the height over which the sediment falls ultimately dictates the duration of the fractionation experiment. Table 1 lists durations and fall heights for some common grain size fractions assuming an average density of quartz ($2.65 \text{ g}\cdot\text{cm}^{-3}$). The finest sediment fraction can be recovered from suspension by using a centrifuge and whether they are sieved or settled different fractions should then be labeled and either freeze dried (preferable) or air dried at room temperature ($\sim 25 \text{ }^\circ\text{C}$) prior to preparation for measurement.

Table 1. Calculated settling times using Equation (1) to calculate fall velocity for a range of particle sizes over six fall heights. Timings are calculated using the density of quartz $2650 \text{ kg}\cdot\text{m}^{-3}$ and the density ($998 \text{ kg}\cdot\text{m}^{-3}$) and viscosity ($1.002 \times 10^{-3} \text{ kg}\cdot\text{m}^{-1}\cdot\text{s}^{-1}$) of water at $20 \text{ }^\circ\text{C}$. “h” = hour(s), “m” = minute(s), “s” = second(s). Micrometer sizes (μm) are given as an approximation of phi (ϕ) size.

Fall Height	31 μm (5 ϕ)	16 μm (6 ϕ)	8 μm (7 ϕ)	4 μm (8 ϕ)	2 μm (9 ϕ)
5 cm	54 s	3 m 37 s	14 m 30 s	58 m 59 s	3 h 52 m
10 cm	1 m 49 s	7 m 15 s	29 m 00 s	1 h 56 m	7 h 44 m
15 cm	2 m 43 s	10 m 52 s	43 m 30 s	2 h 54 m	11 h 36 m
20 cm	3 m 37 s	14 m 30 s	57 m 59 s	3 h 52 m	15 h 28 m
25 cm	4 m 32 s	18 m 07 s	1 h 12 m	4 h 50 m	19 h 20 m
30 cm	5 m 26 s	21 m 45 s	1 h 27 m	5 h 48 m	23 h 12 m

5.3. Magnetic Measurements

Dried sample fractions should be weighed so the granulometric contribution of different particle sizes to the bulk sample can be calculated. Sample measurement cubes, cylinders, capsules, and straws vary between equipment but all packed material should be immobilized and weighed prior to measurement to permit calculation and comparison of magnetic properties on a mass specific basis. To facilitate direct

comparison with the bulk record, it is recommended that the bulk magnetic properties of the sample are either measured prior to separation or some bulk sample is retained to permit bulk measurement alongside the measurement of its fractions. This allows comparison of individual fractions to the bulk sediment and examination of which fraction, or combination of fractions, might be important for driving bulk magnetic properties. This also allows for a test of linear additivity as the sum of the different fractions weighted by their abundance should equal the measurement of the bulk sediment. The suite of magnetic measurements employed will largely be dictated by the specific requirements of the investigation, however, measurements of MS, ARM and/or hysteresis measurements, and IRM at several fields, and calculation of their intra-parametric ratios, should be considered a minimum to characterize the concentration, grain-size, and mineralogy of the magnetic grain assemblage.

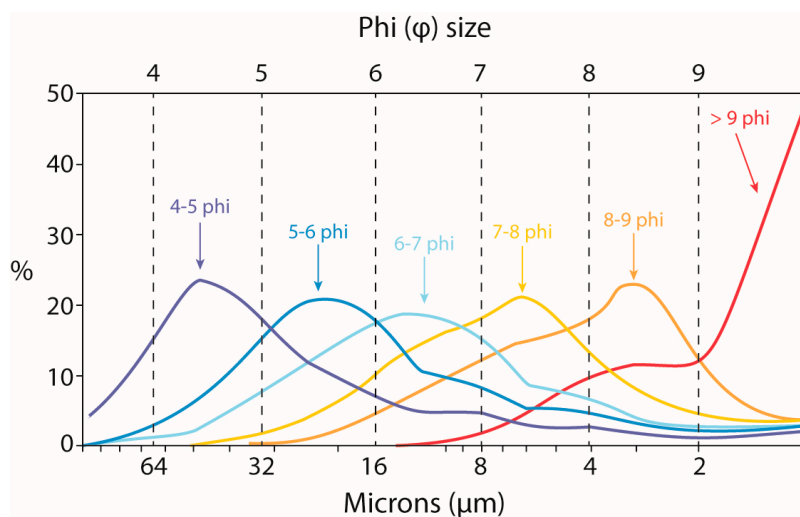
5.4. Limitations of Particle Size Specific Measurements

The discriminatory power of particle size specific measurements inherently relies on different components associating with different size fractions. Isolation of these different fractions then provides a pathway to isolate different magnetic fingerprints. However, if multiple components reside in the same fraction (e.g., diagenetic products and detrital sources) difficulty may exist in discriminating their separate fingerprints using simple particle size specific measurements. If their coercivity spectra differ, the techniques outlined in Section 3 [49–52,114] might be a useful tool to identify the presence of multiple components within the same sedimentary fraction. Making these high resolution measurements on sediment particles size fractions can be increasingly resource intensive, however, if they can identify and link different components within the fraction with their sedimentological abundance in the bulk sediment, they can potentially provide a better estimate and understanding of how the bulk magnetic record is constructed.

In addition to the resource and time constraints that fractionation imparts on data generation several other factors should be noted. Natural sediments are rarely dominated by spherical grains; instead, they often range from close to spherical grains to needle-like rods and platy clays. This can affect how different particles fractionate into different grain size ranges. For example, platy clays have slower settling velocities than spherical particles and a rod shaped particle that could pass through a sieve along one axis might not be able to if it is rotated 90°. While non-spherical induced drag can enrich the finer fractions in coarser sediments, variations in mineralogical density can enrich the coarse fractions in fine particles (Figure 7). For most settling studies, the average density of quartz ($2650 \text{ kg}\cdot\text{m}^{-3}$) is often assumed to generate a settling velocity [11,12,17,18,31,32], however, natural samples often differ from this average value resulting in variations in settling velocity for a given particle size [140,141]. Of considerable importance for magnetic studies is that the density of magnetite ($5170 \text{ kg}\cdot\text{m}^{-3}$) is almost twice that of quartz. While this is not as important for wet sieving of the coarser fractions where grain size binning is purely determined by size, it is especially important for the calculation of fall velocity as discrete magnetite will settle through the sediment column almost twice as fast as similar sized quartz grains. This can result in a finer magnetic population relative to its surrounding sediment matrix which becomes important when comparisons are made between sediment and magnetic grain sizes. For example, quartz dominated silt separated at 7ϕ ($\sim 32 \mu\text{m}$) could contain coarse PSD size discrete magnetite grains at the PSD/MD boundary ($\sim 20 \mu\text{m}$) within a fraction that purely by size should theoretically be dominated by MD size grains.

Consistency in the methodology used can also be a factor that might affect sediment separation. While the use of multiple personnel to assist in sample fractionation certainly speeds up the separation process, different operators are likely to introduce their own bias through slight differences in technique. Similarly, someone learning these techniques may refine and improve their methodology through practice meaning that after several cycles of repetition, later samples may deviate slightly from the first batch of samples processed. While these biases are harder to account for, they should be considered especially if systematic offsets are apparent in the dataset. Ultimately, these assumptions and nuances mean that there is often an observed distribution of particle sizes outside of the targeted range when the particle size distribution of fractionated samples is analyzed (Figure 7, [140,141]). In the experiment, in Figure 7, samples were only settled once, while in practice separation of each fraction is usually repeated at least twice for each fraction [11,12] to reduce contamination by fines in the coarser fractions. When this methodology is applied, the percentage of material in the finer tail is greatly reduced (e.g., [141]) though coarse and fine particles still exist outside the target range. While it is almost impossible to prevent contamination of fines in the coarser fractions—and *vice versa*—ensuring the same techniques are applied to all samples can help minimize separation variances and permit comparison of similar size distributions.

Figure 7. Laser granulometry measurements of the particle size distribution of separated sediment fractions. Note that the mode occurs within the target range but it accompanied by large tails overlapping into different particle size bins. The coarser fractions are more positively skewed being enriched in fines, while the fines are more negatively skewed being enriched in coarser grains. Figure redrawn from Walden and Slattery [140].



6. Summary and Future Directions

Measurement of particle size-specific magnetic properties demonstrates great potential for understanding the drivers of the bulk magnetic record. This methodology allows a determination of how magnetic minerals and magnetic grain sizes are carried in the bulk sediment, which sediment grain sizes they associate with, how sedimentology affects bulk magnetic properties, to what extent the simple relationship between sediment and magnetic grain size can be assumed, and what processes and/or sources likely affect variances in the bulk magnetic record. Through isolation of specific fractions,

certain components can also be amplified and/or cleaned from the study. However, compared to bulk measurements, their generation is time consuming and while not sample destructive they are sample intrusive. This may be a major barrier in studies that utilize magnetic properties because of their rapid, non-destructive nature. As a compromise, an appropriate methodology might be to employ a pilot study to examine the degree of particle size dependence in a few representative samples and examine if bulk magnetic properties can be better understood and interpreted from these pilot data. This approach has been successfully applied in a range of environments, for example, to understand the deposition of silt-size pollution derived magnetic spherules [3,13–15], the generation of ultra-fine magnetite through pedogenesis [3,31,67,77], concentration of heavy magnetic minerals as placer deposits in zones of erosion [123,142], and to understand variations in source and sediments (Figures 4 and 5, [10,32,128]). Alternatively, the pilot study might reveal that particle size specific magnetic measurements are necessary to target reveal certain aspects of the record (e.g., Figure 6) and in these cases they often reveal information that could not otherwise have been gained through measurement of bulk magnetic properties.

Although particle size specific measurements are becoming more frequently employed in the literature, their number is still small in relation to the generation of bulk magnetic records. From this standpoint, particle size specific measurement is very much still in its infancy, despite being used for over 30 years (e.g., [30,69,121]), and the more studies that make these types of measurements the more questions they often produce. Why magnetic fragments partition with different fractions is an important but not fully understood question. In some cases, it appears relatively simple and is related to the presence of discrete magnetic particles, in other situations the hosting of magnetic particles as inclusions may make interpretation more complex (e.g., [32]). How and why magnetic material is hosted within polycrystalline clasts and how they are subsequently weathered into a range of discrete and/or included magnetic particles is also poorly understood. This may be related to host rock type, cooling rate, and/or the nature of the weathering but is yet to be fully investigated. Some rock types may be more preconditioned to release discrete magnetic grains during weathering, while others may be better equipped to retain the non-magnetic matrix magnetic grains that are contained within. This has important implications for the interpretation of bulk magnetic properties and how we view the relationship between sediment and magnetic grain size.

Aside from the tentative suggestion that 3 μm might be the optimal boundary to separate pedogenic SP grains [31], there are at present no criteria that might assist with distinguishing the optimal number of sediment fractions and ranges for separation from the bulk sediment sample. Most sediment size separations are based on additional information and sometimes just scientific instinct. The development of a protocol to best target, select, and isolate different components within the bulk signal would be a useful step and might highlight certain fractions that appear important for hosting bulk magnetic properties. A better protocol to assist separations, and even define the most optimal ranges to use, will not only assist in making the separation process more efficient, but will aid comparison of the same size fractions between studies. With an increased number of particle size-specific records using common fractionation strategies, some of the more fundamental magnetic questions can begin to be addressed rather than just exploiting particle size-specific measurements to answer specific research questions. These broader impacts have not only implications for the drivers of the bulk environmental magnetic record but also for how magnetic recording occurs in sediment paleomagnetic records which demand interpretation of the undisturbed bulk magnetic sediment.

Acknowledgments

Robert G. Hatfield would like to acknowledge support from the National Science Foundation through a Paleo Perspectives on Climate Change Grant ARC-0902751 to Joseph S. Stoner and Anders E. Carlson and an Ocean Drilling Program Grant OCE-1260671 to Robert G. Hatfield and Joseph S. Stoner. Robert G. Hatfield would also like to thank Barbara Maher, Maria Cioppa, and Joseph Stoner for training, guidance, conversations, and support during investigations into the particle size dependence of magnetic properties and three reviewers who greatly improved this manuscript.

Conflicts of Interest

The author declares no conflict of interest.

References

1. Thompson, R.; Battarbee, R.W.; O'Sullivan, P.E.; Oldfield, F. Magnetic susceptibility of lake sediments. *Limnol. Oceanogr.* **1975**, *20*, 687–698.
2. Thompson, R.; Oldfield, F. *Environmental Magnetism*; Allen & Unwin: London, UK, 1986.
3. Maher, B.A. Characterisation of soils by mineral magnetic measurements. *Phys. Earth Planet. Inter.* **1986**, *42*, 76–92.
4. Robinson, S.G. The late Pleistocene palaeoclimatic record of North Atlantic deep-sea sediments revealed by mineral-magnetic measurements. *Phys. Earth Planet. Inter.* **1986**, *42*, 22–47.
5. Maher, B.A.; Thompson, R. Mineral magnetic record of the Chinese loess and paleosols. *Geology* **1991**, *19*, 3–6.
6. Maher, B.A.; Thompson, R. Paleoclimatic significance of the mineral magnetic record of the Chinese loess and paleosols. *Quat. Res.* **1992**, *37*, 155–170.
7. Grousset, F.E.; Labeyrie, L.; Sinko, J.A.; Cremer, M.; Bond, G.; Duprat, J.; Cortijo, E.; Huon, S. Patterns of ice-rafted detritus in the glacial North Atlantic (40–55° N). *Paleoceanography* **1993**, *8*, 175–192.
8. Rasmussen, T.L.; van Weering, T.C.E.; Labeyrie, L. Climatic instability, ice sheets and ocean dynamics at high northern latitudes during the last glacial period (58–10 KA BP). *Quat. Sci. Rev.* **1997**, *16*, 71–80.
9. Kissel, C.; Laj, C.; Labeyrie, L.; Dokken, T.; Voelker, A.; Blamart, D. Rapid climatic variations during marine isotopic stage 3: Magnetic analysis of sediments from Nordic Seas and North Atlantic. *Earth Planet. Sci. Lett.* **1999**, *171*, 489–502.
10. Rosenbaum, J.G.; Reynolds, R.L. Basis for paleoenvironmental interpretation of magnetic properties of sediment from upper Klamath lake (Oregon): Effects of weathering and mineralogical sorting. *J. Paleolimnol.* **2004**, *31*, 253–265.
11. Hatfield, R.G.; Maher, B.A. Suspended sediment characterization and tracing using a magnetic fingerprinting technique: Bassenthwaite Lake, Cumbria, UK. *Holocene* **2008**, *18*, 105–115.

12. Razik, S.; Dekkers, M.J.; von Dobeneck, T. How environmental magnetism can enhance the interpretational value of grain-size analysis: A time-slice study on sediment export to the NW African margin in Heinrich Stadial 1 and Mid Holocene. *Palaeogeogr. Palaeoclimatol. Palaecol.* **2014**, *406*, 33–48.
13. Kapička, A.; Petrovský, E.; Ustjakk, S.; Macháčková, K. Proxy mapping of fly-ash pollution of soils around a coal-burning power plant: A case study in the Czech Republic. *J. Geochem. Explor.* **1999**, *66*, 291–297.
14. Hoffmann, V.; Knab, M.; Appel, E. Magnetic susceptibility mapping of roadside pollution. *J. Geochem. Explor.* **1999**, *66*, 313–326.
15. Hansard, R.; Maher, B.A.; Kinnersley, R. Biomagnetic monitoring of industry-derived particulate pollution. *Environ. Pollut.* **2011**, *159*, 1673–1681.
16. Walling, D.E.; Peart, M.R.; Oldfield, F.; Thompson, R. Suspended sediment sources identified by magnetic measurements. *Nature* **1979**, *281*, 110–113.
17. Hatfield, R.G.; Maher, B.A. Holocene sediment dynamics in an upland temperate catchment: Climatic and land-use impacts in the English Lake District. *Holocene* **2009**, *19*, 427–438.
18. Hatfield, R.G.; Maher, B.A.; Pates, J.M.; Barker, P.A. Sediment dynamics in an upland temperate catchment: Changing sediment sources, rates, and deposition. *J. Paleolimnol.* **2008**, *40*, 1143–1158.
19. Maher, B.A.; Thompson, R.; Zhou, L.P. Spatial and temporal reconstructions of changes in the Asian palaeomonsoon: A new mineral magnetic approach. *Earth Planet. Sci. Lett.* **1994**, *125*, 461–471.
20. Maher, B.A.; Hu, M.; Roberts, H.M.; Wintle, A.G. Holocene loess accumulation and soil development at the western edge of the Chinese Loess Plateau: Implications for magnetic proxies of paleorainfall. *Quat. Sci. Rev.* **2002**, *22*, 445–451.
21. Geiss, C.E.; Egli, R.; Zanner, C.W. Direct estimates of pedogenic magnetite as a tool to reconstruct past climates from buried soils. *J. Geophys. Res.* **2008**, *113*, 1–15.
22. Stoner, J.S.; Channell, J.E.T.; Hillaire-Marcel, C. The magnetic signature of rapidly deposited detrital layers from the Deep Labrador Sea: Relationship to North Atlantic Heinrich layers. *Paleoceanography* **1996**, *11*, 309–325.
23. Watkins, S.J.; Maher, B.A. Magnetic characterisation of present-day deep-sea sediments and sources in the North Atlantic. *Earth Planet. Sci. Lett.* **2003**, *214*, 379–394.
24. Bloemendal, J.; de Menocal, P. Evidence for a change in the periodicity of tropical climate cycles at 2.4 Myr from whole-core magnetic susceptibility measurements. *Nature* **1989**, *342*, 897–900.
25. Stoner, J.S.; Channell, J.E.T.; Hillaire-Marcel, C. Magnetic properties of deep—Sea sediments off southwest Greenland: Evidence for major differences between the last two deglaciations. *Geology* **1995**, *23*, 241–244.
26. Kissel, C.; Laj, C.; Mulder, T.; Wandres, C.; Cremer, M. The magnetic fraction: A tracer of deep water circulation in the North Atlantic. *Earth Planet. Sci. Lett.* **2009**, *288*, 444–454.
27. Snowball, I.; Moros, M. Saw-tooth pattern of North Atlantic current speed during Dansgaard-Oeschger cycles revealed by the magnetic grain size of Reykjanes Ridge sediments at 59° N. *Paleoceanography* **2003**, *18*, 1026–1037.
28. Ballini, M.; Kissel, C.; Colin, C.; Richter, T. Deep-water mass source and dynamic associated with rapid climatic variations during the last glacial stage in the North Atlantic: A multiproxy investigation of the detrital fraction of deep-sea sediments. *Geochem. Geophys. Geosyst.* **2006**, *7*, Q02N01.

29. Heller, F.; Liu, T.S. Palaeoclimatic and sedimentary history from magnetic susceptibility of loess in China. *Geophys. Res. Lett.* **1986**, *13*, 1169–1172.
30. Oldfield, F.; Maher, B.A.; Donoghue, J.; Pierce, J. Particle-size related mineral magnetic source sediment linkages in the Rhode River catchment, Maryland, USA. *J. Geol. Soc.* **1985**, *142*, 1035–1046.
31. Oldfield, F.; Hao, Q.; Bloemendal, J.; Gibbs-Eggar, Z.; Patil, S.; Guo, Z. Links between bulk sediment particle size and magnetic grain size: General observations and implications for Chinese loess studies. *Sedimentology* **2009**, *56*, 2091–2106.
32. Hatfield, R.G.; Stoner, J.S.; Carlson, A.E.; Reyes, A.V.; Housen, B. Source as a controlling factor on the quality and interpretation of sediment magnetic records from the northern North Atlantic. *Earth Planet. Sci. Lett.* **2013**, *368*, 69–77.
33. Canfield, D.E.; Berner, R.A. Dissolution and pyritization of magnetite in anoxic marine sediments. *Geochim. Cosmochim. Acta* **1987**, *51*, 645–659.
34. Roberts, A.P.; Turner, G.M. Diagenetic formation of ferrimagnetic iron sulphide minerals in rapidly deposited marine sediments, South Island, New Zealand. *Earth Planet. Sci. Lett.* **1993**, *115*, 257–273.
35. Passier, H.F.; Dekkers, M.J. Iron oxide formation in the active oxidation front above sapropel S1 in the eastern Mediterranean Sea as derived from low-temperature magnetism. *Geophys. J. Int.* **2002**, *150*, 230–240.
36. Larrasoaña, J.C.; Roberts, A.P.; Musgrave, R.J.; Gràcia, E.; Piñero, P.; Vega, M.; Martínez-Ruiz, F. Diagenetic formation of greigite and pyrrhotite in gas hydrate marine sedimentary systems. *Earth Planet. Sci. Lett.* **2007**, *261*, 350–366.
37. Rowan, C.J.; Roberts, A.P.; Broadbent, T. Reductive diagenesis, magnetite dissolution, greigite growth and paleomagnetic smoothing in marine sediments: A new view. *Earth Planet. Sci. Lett.* **2009**, *277*, 223–235.
38. Maher, B.A.; Taylor, R.M. Formation of ultrafine-grained magnetite in soils. *Nature* **1988**, *336*, 368–370.
39. Snowball, I.F. Bacterial magnetite and the magnetic properties of sediments in a Swedish lake. *Earth Planet. Sci. Lett.* **1994**, *126*, 129–142.
40. Yamazaki, T. Magnetostatic interactions in deep-sea sediments inferred from first-order reversal curve diagrams: Implications for relative paleointensity normalization. *Geochem. Geophys. Geosyst.* **2008**, *9*, Q02005, doi:10.1029/2007GC001797.
41. Robinson, S.G.; Maslin, M.A.; McCave, I.N. Magnetic susceptibility variations in Upper Pleistocene deep-sea sediments of the NE Atlantic: Implications for ice rafting and paleocirculation at the last glacial maximum. *Paleoceanography* **1995**, *10*, 221–250.
42. Zhang, W.; Yu, L.; Lu, M.; Hutchinson, S.; Feng, H. Magnetic approach to normalizing heavy metal concentrations for particle size effects in intertidal sediments in the Yangtze Estuary, China. *Environ. Pollut.* **2007**, *147*, 238–244.
43. Karlin, R.; Levi, S. Diagenesis of magnetic minerals in recent haemipelagic sediments. *Nature* **1983**, *303*, 327–330.
44. Karlin, R.; Levi, S. Geochemical and sedimentological control of the magnetic properties of hemipelagic sediments. *J. Geophys. Res.* **1985**, *90*, 10373–10392.

45. Robinson, S.G.; Sahota, J.T.S.; Oldfield, F. Early diagenesis in North Atlantic abyssal plain sediments characterized by rock-magnetic and geochemical indices. *Mar. Geol.* **2000**, *163*, 77–107.
46. Russell, M.A.; Walling, D.E.; Hodgkinson, R.A. Suspended sediment sources in two small lowland agricultural catchments in the UK. *J. Hydrol.* **2001**, *252*, 1–24.
47. Robertson, D.J.; France, D.E. Discrimination of remanence-carrying minerals in mixtures using isothermal remanent magnetization acquisition curves. *Phys. Earth Planet. Inter.* **1994**, *82*, 223–234.
48. Heslop, D.; Dekkers, M.J.; Kruiver, P.P.; van Oorschot, I.H.M. Analysis of isothermal remanent magnetization acquisition curves using the expectation—Maximization algorithm. *Geophys. J. Int.* **2002**, *148*, 58–64.
49. Egli, R. Analysis of the field dependence of remanent magnetization curves. *J. Geophys. Res.* **2003**, *108*, 2081, doi:10.1029/2002JB002023.
50. Egli, R. Characterization of individual rock magnetic components by analysis of remanence curves. 1. Unmixing natural sediments. *Stud. Geophys. Geod.* **2004**, *48*, 391–446.
51. Egli, R. Characterization of individual rock magnetic components by analysis of remanence curves. 2. Fundamental properties of coercivity distributions. *Phys. Chem. Earth* **2004**, *29*, 851–867.
52. Egli, R. Characterization of individual rock magnetic components by analysis of remanence curves. 3. Bacterial magnetite and natural processes in lakes. *Phys. Chem. Earth* **2004**, *29*, 869–884.
53. Lascu, I.; Banerjee, S.K.; Berquo, T.S. Quantifying the concentration of ferrimagnetic particles in sediments using rock magnetic methods. *Geochem. Geophys. Geosyst.* **2010**, *11*, Q08Z19, doi:10.1029/2010GC003182.
54. Heslop, D.; Roberts, A.P. Estimating best fit binary mixing lines in the Day plot. *J. Geophys. Res.* **2012**, *117*, B01101, doi:10.1029/2011JB008787.
55. Heslop, D.; Roberts, A.P. A method for unmixing magnetic hysteresis loops. *J. Geophys. Res.* **2012**, *117*, B03103, doi:10.1029/2011JB008859.
56. Evans, M.E.; Heller, F. *Environmental Magnetism: Principles and Applications of Enviromagnetics*; Academic Press: London, UK, 2003.
57. Dekkers, M.J. Magnetic proxy parameters. In *Encyclopedia of Geomagnetism and Paleomagnetism*; Gubbins, D., Herrero-Bervera, E., Eds.; Springer: Amsterdam, The Netherlands, 2007.
58. Dunlop, D.J.; Ozdemir, O. *Rock Magnetism. Fundamentals and Frontiers*; Cambridge University Press: Cambridge, UK, 2001.
59. Kletetschka, G.; Wasilewski, P.J. Grain size limit for SD hematite. *Phys. Earth Planet. Inter.* **2002**, *129*, 173–179.
60. Thompson, R. Modelling magnetization data using SIMPLEX. *Phys. Earth Planet. Inter.* **1986**, *42*, 113–127.
61. Gee, J.; Kent, D.V. Calibration of magnetic granulometric trends in oceanic basalts. *Earth Planet. Sci. Lett.* **1999**, *170*, 377–390.
62. Stanford, J.D.; Rohling, E.J.; Hunter, S.E.; Roberts, A.P.; Rasmussen, S.O.; Bard, E.; McManus, J.; Fairbanks, R.G. Timing of meltwater pulse 1a and climate responses to meltwater injections. *Paleoceanography* **2006**, *21*, PA4103.
63. Maher, B.A.; Thompson, R. *Quaternary Climates, Environments and Magnetism*; Cambridge University Press: Cambridge, UK, 1999.

64. Butler, R.F. *Paleomagnetism: Magnetic Domains to Geologic Terranes*; Blackwell: London, UK, 1992.
65. Zhou, W.; van der Voo, R.; Peacor, D.R.; Zhang, Y. Variable Ti-content and grain size of titanomagnetite as a function of cooling rate in very young MORB. *Earth Planet. Sci. Lett.* **2000**, *179*, 9–20.
66. Maher, B.A. Magnetic properties of some synthetic sub-micron magnetites. *Geophys. J. R. Astron. Soc.* **1988**, *94*, 83–96.
67. Maher, B.A. Magnetic properties of modern soils and loessic paleosols: Implications for paleoclimate. *Palaeogeogr. Palaeoclimatol. Palaeocol.* **1998**, *137*, 25–54.
68. Grimley, D.A.; Arruda, N.K.; Bramstedt, M.W. Using magnetic susceptibility to facilitate more rapid, reproducible and precise delineation of hydric soils in the midwestern USA. *Catena* **2004**, *58*, 183–213.
69. Yu, L.; Oldfield, F. Quantitative sediment source ascription using magnetic measurements in a reservoir-catchment system near Nijar, S.E. Spain. *Earth Surf. Process. Landf.* **1993**, *18*, 441–454.
70. Caitcheon, G.G. Applying environmental magnetism to sediment tracing. In *Tracers in Hydrology*; International Association of Hydrological Sciences Publication No. 215; Peters, N.E., Hoehn, E., Leibundgut, C., Tase, N., Walling, D.E., Eds.; IAHS Press: Wallingford, UK, 1993; pp. 285–292.
71. Roberts, A.P. Magnetic characteristics of sedimentary greigite (Fe₃S₄). *Earth Planet. Sci. Lett.* **1995**, *134*, 227–236.
72. Rowan, C.J.; Roberts, A.P. Magnetite dissolution, diachronous greigite formation, and secondary magnetizations from pyrite oxidation: Unravelling complex magnetizations in Neogene marine sediments from New Zealand. *Earth Planet. Sci. Lett.* **2006**, *241*, 119–137.
73. Roberts, A.P.; Chang, L.; Rowan, C.J.; Horng, C.-S.; Florindo, F. Magnetic properties of sedimentary greigite (Fe₃S₄): An update. *Rev. Geophys.* **2011**, *49*, RG1002, doi: 10.1029/2010RG000336.
74. Kent, D.V.; Lowrie, W. Origin of magnetic instability in sediment cores from the Central North Pacific. *J. Geophys. Res.* **1974**, *79*, 2987–3000.
75. Passier, H.F.; de Lange, G.J.; Dekkers, M.J. Rock-magnetic properties and geochemistry of the active oxidation front and the youngest sapropel in the eastern Mediterranean. *Geophys. J. Int.* **2001**, *145*, 604–614.
76. Dearing, J.A.; Dann, R.J.L.; Hay, K.; Lees, J.A.; Loveland, P.J.; Maher, B.A.; O'Grady, K. Frequency-dependant susceptibility measurements of environmental materials. *Geophys. J. Int.* **1996**, *124*, 228–240.
77. Zheng, H.; Oldfield, F.; Yu, L.; Shaw, J.; An, Z. The magnetic properties of particle-sized samples from the Luo Chuan loess section: Evidence for pedogenesis. *Phys. Earth Planet. Inter.* **1991**, *68*, 250–258.
78. Blakemore, R. Magnetotactic bacteria. *Science* **1975**, *190*, 377–379.
79. Petersen, N.; von Dobeneck, T.; Vali, H. Fossil bacterial magnetite in deep-sea sediments from the South Atlantic Ocean. *Nature* **1986**, *320*, 611–615.
80. Kopp, R.E.; Kirschvink, J.L. The identification and biogeochemical interpretation of fossilized magnetotactic bacteria. *Earth Sci. Rev.* **2008**, *86*, 42–61.
81. Kirschvink, J.L.; Chang, S.R. Ultrafine-grained magnetite in deep-sea sediments: Possible bacterial magnetofossils. *Geology* **1984**, *12*, 559–562.

82. Paasche, Ø.; Løvlie, R.; Dahl, S.O.; Bakke, J.; Nesje, A. Bacterial magnetite in lake sediments: Late glacial to Holocene climate and sedimentary changes in northern Norway. *Earth Planet. Sci. Lett.* **2004**, *223*, 319–333.
83. Shen, Z.; Bloemendal, J.; Mauz, B.; Chiverrall, R.C.; Dearing, J.A.; Lang, A.; Liu, Q. Holocene environmental reconstruction of sediment-source linkages at Crummock Water, English Lake District, based on magnetic measurements. *Holocene* **2008**, *18*, 129–140.
84. Egli, R. VARIFORC: An optimized protocol for calculating non-regular first-order reversal curve (FORC) diagrams. *Glob. Planet. Chang.* **2013**, *110*, 302–320.
85. Harrison, R.J.; Feinberg, J.M. FORCinel: An improved algorithm for calculating first-order reversal curve distributions using locally weighted regression smoothing. *Geochem. Geophys. Geosyst.* **2008**, *9*, Q05016.
86. Roberts, A.P.; Pike, C.R.; Verosub, K.L. First-order reversal curve diagrams: A new tool for characterizing the magnetic properties of natural samples. *J. Geophys. Res.* **2000**, *105*, 28461–28475.
87. Chen, A.P.; Egli, R.; Moskowitz, B.M. First-order reversal curve (FORC) diagrams of natural and cultured biogenic magnetic particles. *J. Geophys. Res.* **2007**, *112*, B08S90.
88. Hanesch, M.; Scholger, R. The influence of soil type on the magnetic susceptibility measured throughout soil profiles. *Geophys. J. Int.* **2005**, *161*, 50–56.
89. Mitchell, R.; Maher, B.A.; Kinnersley, R. Rates of particulate pollution deposition onto leaf surfaces: Temporal and inter-species analyses. *Environ. Pollut.* **2010**, *158*, 1472–1478.
90. Hanesch, M.; Scholger, R. Mapping of heavy metal loadings in soils by means of magnetic susceptibility measurements. *J. Environ. Geol.* **2002**, *42*, 857–870.
91. Shi, R.; Cioppa, M. Magnetic survey of topsoils in Windsor-Essex County, Canada. *J. Appl. Geophys.* **2006**, *60*, 201–212.
92. Day, R.; Fuller, M.; Schmidt, V.A. Hysteresis properties of titanomagnetites: Grain size and composition dependence. *Phys. Earth Planet. Inter.* **1977**, *13*, 260–267.
93. Dunlop, D.J. Theory and application of the Day plot (Mrs/Ms versus Hcr/Hc): 1. Theoretical curves and tests using titanomagnetite data. *J. Geophys. Res.* **2002**, *107*, doi:10.1029/2001JB000486.
94. Dunlop, D.J. Theory and application of the Day plot (Mrs/Ms versus Hcr/Hc): 2. Application to data for rocks, sediments, and soils. *J. Geophys. Res.* **2002**, *107*, doi:10.1029/2001JB000487.
95. Oldfield, F. Toward the discrimination of fine-grained ferrimagnets by magnetic measurements in lake and near-shore marine sediments. *J. Geophys. Res.* **1994**, *99*, 9045–9050.
96. Oldfield, F. Sources of fine-grained magnetic minerals in sediments: A problem revisited. *Holocene* **2007**, *17*, 1265–1271.
97. Van der Post, K.D.; Oldfield, F.; Haworth, E.Y.; Crooks, P.R.J.; Appleby, P.G. A record of accelerated erosion in the recent sediments of Blelham Tarn in the English Lake District. *J. Paleolimnol.* **1997**, *18*, 103–120.
98. Peters, C.; Dekkers, M.J. Selected room temperature magnetic parameters as a function of mineralogy, concentration and grain size. *Phys. Chem. Earth* **2003**, *28*, 659–667.
99. Lees, J.A. Mineral magnetic properties of mixtures of environmental and synthetic materials: Linear additivity and interaction effects. *Geophys. J. Int.* **1997**, *131*, 335–346.

100. Lees, J.A. Evaluating magnetic parameters for use in source identification, classification and modelling of natural and environmental materials. In *Environmental Magnetism: A Practical Guide*; Technical Guide No. 6; Oldfield, F., Walden, J., Smith, J., Eds.; Quaternary Research Association: London, UK, 1999; pp. 113–138.
101. Lascu, I.; McLauchlan, K.K.; Myrbo, A.; Leavitt, P.R.; Banerjee, S.K. Sediment-magnetic evidence for last millennium drought conditions at the prairie—Forest ecotone of northern United States. *Palaeogeogr. Palaeoclimatol. Palaeocol.* **2012**, *337*, 99–107.
102. Lees, J.A. Modelling the Magnetic Properties of Natural and Environmental Materials. Ph.D. Thesis, Coventry University, Coventry, UK, 1994.
103. Rowan, J.S.; Goodwill, P.; Franks, S.W. Uncertainty estimation in fingerprinting suspended sediment sources. In *Tracers in Geomorphology*; Foster, I.D.L., Ed.; Wiley: Chichester, UK, 2000; pp. 279–290.
104. Stockhausen, H. Some new aspects for the modelling of isothermal remanent magnetization acquisition curves by cumulative log Gaussian functions. *Geophys. Res. Lett.* **1998**, *25*, 2217–2220.
105. Kruiver, P.P.; Dekkers, M.J.; Heslop, D. Quantification of magnetic coercivity components by the analysis of acquisition curves of isothermal remanent magnetization. *Earth Planet. Sci. Lett.* **2001**, *189*, 269–276.
106. Heslop, D.; McIntosh, G.; Dekkers, M.J. Using time and temperature dependant Preisach models to investigate the limitations of modelling isothermal remanent magnetization acquisition curves with cumulative log Gaussian functions. *Geophys. J. Int.* **2004**, *157*, 55–63.
107. Spassov, S.; Egli, R.; Heller, F.; Nourgaliev, D.K.; Hannam, J. Magnetic quantification of urban pollution sources in atmospheric particulate matter. *Geophys. J. Int.* **2004**, *159*, 555–564.
108. Sagnotti, L.; Macri, P.; Egli, R.; Mondino, M. Magnetic properties of atmospheric particulate matter from automatic air sampler stations in Latium (Italy): Toward a definition of magnetic fingerprints for natural and anthropogenic PM10 sources. *J. Geophys. Res.* **2006**, *111*, B12S22, doi:10.1029/2006JB004508.
109. Yamazaki, T. Paleoposition of Intertropical Convergence Zone in the eastern Pacific inferred from glacial-interglacial changes in terrigenous and biogenic magnetic mineral fractions. *Geology* **2012**, *40*, 151–154.
110. Chang, L.; Winklhofer, M.; Roberts, A.P.; Heslop, D.; Florindo, F.; Dekkers, M.J.; Krijgsman, W.; Kodama, K.; Yamamoto, Y. Low-temperature magnetic properties of pelagic carbonates: Oxidation of biogenic magnetite and identification of magnetosome chains. *J. Geophys. Res. Sol. Earth* **2013**, *118*, 6049–6065.
111. Jackson, M.; Solheid, P. On the quantitative analysis and evaluation of magnetic hysteresis data. *Geochem. Geophys. Geosyst.* **2010**, *11*, Q04Z15, doi:10.1029/2009GC002932.
112. Pike, C.R.; Roberts, A.P.; Verosub, K.L. Characterizing interactions in fine magnetic particle systems using first order reversal curves. *J. Appl. Phys.* **1999**, *85*, 6660–6667.
113. Roberts, A.P.; Pike, C.R.; Verosub, K.L. First-order reversal curve diagrams and thermal relaxation effects in magnetic particles. *Geophys. J. Int.* **2001**, *145*, 721–730.
114. Egli, R.; Chen, A.P.; Winklhofer, M.; Kodama, K.P.; Horng, C.-S. Detection of noninteracting single domain particles using first-order reversal curve diagrams. *Geochem. Geophys. Geosyst.* **2010**, *11*, Q01Z11, doi:10.1029/2009GC002916.

115. Carter-Stiglitz, B.; Moskowitz, B.; Jackson, M. Unmixing magnetic assemblages and the magnetic behavior of bimodal mixtures. *J. Geophys. Res.* **2001**, *106*, 26397–26412.
116. Yu, Y.; Dunlop, D.J.; Özdemir, Ö. Partial anhysteretic remanent magnetization in magnetite, 1: Additivity. *J. Geophys. Res.* **2002**, *107*, B001249, doi:10.1029/2001JB001249.
117. Channell, J.E.T.; Hodell, D.A.; Lehman, B. Relative geomagnetic paleointensity and $\delta^{18}\text{O}$ at ODP Site 983 (Gardar Drift, North Atlantic) since 350 ka. *Earth Planet. Sci. Lett.* **1997**, *153*, 103–118.
118. Channell, J.E.T. Geomagnetic paleointensity and directional secular variation at Ocean Drilling Program (ODP) Site 984 (Bjorn Drift) since 500 ka: Comparisons with ODP Site 983 (Gardar Drift). *J. Geophys. Res.* **1999**, *104*, 22937–22951.
119. Evans, H.F.; Channell, J.E.T.; Stoner, J.S.; Hillaire-Marcel, C.; Wright, J.D.; Neitzke, L.C.; Mountain, G.S. Paleointensity-assisted chronostratigraphy of detrital layers on the Eirik Drift (North Atlantic) since marine isotope stage 11. *Geochem. Geophys. Geosyst.* **2007**, *8*, Q11007, doi:10.1029/2007GC001720.
120. Mazaud, A.; Channell, J.E.T.; Stoner, J.S. Relative paleointensity and environmental magnetism since 1.2 Ma at IODP site U1305 (Eirik Drift, NW Atlantic). *Earth Planet. Sci. Lett.* **2012**, *357–358*, 137–144.
121. Oldfield, F.; Yu, L. The influence of particle size variations on the magnetic properties of sediments from the north-eastern Irish Sea. *Sedimentology* **1994**, *41*, 1093–1108.
122. Hao, Q.; Oldfield, F.; Bloemendal, J.; Guo, Z. Particle size separation and evidence for pedogenesis in samples from the Chinese Loess Plateau spanning the last 22 Ma. *Geology* **2008**, *36*, 727–730.
123. Hatfield, R.G.; Cioppa, M.T.; Trenhaile, A.S. Sediment sorting and beach erosion along a coastal foreland: Magnetic measurements in Point Pelee National Park, Ontario, Canada. *Sediment. Geol.* **2010**, *231*, 63–73.
124. Jakobsson, S.P. Chemistry and distribution pattern of recent basaltic rocks in Iceland. *Lithos* **1972**, *5*, 365–386.
125. Andrews, J.T.; Hardardóttir, J.; Stoner, J.S.; Principato, S.M. Holocene sediment magnetic properties along a transect from Ísafjardardjúp to Djúpáll, Northwest Iceland. *Arct. Antarct. Alp. Res.* **2008**, *40*, 1–15.
126. Willigers, B.J.A.; Krogstad, E.J.; Wijbrans, J.R. Comparison of thermochronometers in a slowly cooled granulite Terrain: Nagssugtoqidian Orogen, West Greenland. *J. Petrol.* **2001**, *42*, 1729–1749.
127. Willigers, B.J.A.; van Gool, J.A.M.; Wijbrans, R.; Krogstad, J.; Mezger, K. Posttectonic cooling of the Nagssugtoqidian orogen and a comparison of contrasting cooling histories in Precambrian and Phanerozoic orogens. *J. Geol.* **2002**, *110*, 503–517.
128. Rosenbaum, J.G.; Reynolds, R.L.; Colman, S.M. Fingerprinting of glacial silt in lake sediments yields continuous records of alpine glaciation (35–15 ka), western USA. *Quat. Res.* **2012**, *78*, 333–340.
129. McCave, I.N.; Manighetti, B.; Robinson, S.G. Sortable silt and fine sediment size/composition slicing: Parameters for palaeocurrent speed and palaeoceanography. *Paleoceanography* **1995**, *10*, 593–610.
130. Fagel, N.; Hillaire-Marcel, C.; Humblet, M.; Brasseur, R.; Weis, D.; Stevenson, R. Nd and Pb isotope signatures of the clay-size fraction of Labrador Sea sediments during the Holocene: Implications for the inception of the modern deep circulation pattern. *Paleoceanography* **2004**, *19*, PA3002, doi:10.1029/2003PA000993.

131. Praetorius, S.K.; McManus, J.F.; Oppo, D.W.; Curry, W.B. Episodic reductions in bottom-water currents since the last ice age. *Nat. Geosci.* **2008**, *1*, 449–452.
132. Liu, J.; Zhu, R.; Roberts, A.P.; Li, S.; Chang, J.-H. High-resolution analysis of early diagenetic effects on magnetic minerals in post-middle-Holocene continental shelf sediments from the Korea Strait. *J. Geophys. Res.* **2004**, *109*, B03103.
133. Li, Y.-X.; Yu, Z.; Kodama, K.P.; Moeller, R.E. A 14,000-year environmental change history revealed by mineral magnetic data from White Lake, New Jersey, USA. *Earth Planet. Sci. Lett.* **2006**, *246*, 27–40.
134. Abbott, M.B.; Edwards, M.E.; Finney, B.P. A 40,000-yr record of environmental change from Burial Lake in Northwest Alaska. *Quat. Res.* **2010**, *74*, 156–165.
135. Balascio, N.L.; Bradley, R.S. Evaluating Holocene climate change in northern Norway using sediment records from two contrasting lake systems. *J. Paleolimnol.* **2012**, *48*, 259–273.
136. Wang, Y.; Yu, Z.; Li, G.; Oguchi, T.; He, H.; Shen, H. Discrimination in magnetic properties of different-sized sediments from the Changjiang and Huanghe Estuaries of China and its implication for provenance of sediment on the shelf. *Mar. Geol.* **2009**, *260*, 121–129.
137. Wang, Y.; Dong, H.; Li, G.; Zhang, W.; Oguchi, T.; Bao, M.; Jiang, H.; Bishop, M.E. Magnetic properties of muddy sediments on the northeastern continental shelves of China: Implications for provenance and transportation. *Mar. Geol.* **2010**, *274*, 107–119.
138. Bush, D.C.; Jenkins, R.E.; McCaleb, S.B. Separation of swelling clay minerals by a centrifugal method. *Clays Clay Miner.* **1966**, *14*, 407–418.
139. Smith, J.P. Mineral Magnetic Studies on Two Shropshire-Cheshire Meres. Ph.D. Thesis, University of Liverpool, Liverpool, UK, 1985.
140. Walden, J.; Slattery, M.C. Verification of a simple gravity technique for separation of particle size fractions suitable for mineral magnetic analyses. *Earth Surf. Process. Landf.* **1993**, *18*, 829–833.
141. Clifton, J.; McDonald, P.; Plater, A.; Oldfield, F. An investigation into the efficiency of particle size separation using Stokes' law. *Earth Surf. Process. Landf.* **1999**, *24*, 725–730.
142. Gallaway, E.; Trenhaile, A.S.; Cioppa, M.T.; Hatfield, R.G. Magnetic mineral transport and sorting in the swash-zone: Northern Lake Erie, Canada. *Sedimentology* **2012**, *59*, 1718–1734.